HHS Public Access

Author manuscript

J Am Soc Nephrol. Author manuscript; available in PMC 2015 September 24.

Published in final edited form as:

J Am Soc Nephrol. 2010 November ; 21(11): 1835–1841. doi:10.1681/ASN.2010040378.

A High-Powered View of the Filtration Barrier

János Peti-Peterdi and **Arnold Sipos**

Departments of Physiology and Biophysics and Medicine, Zilkha Neurogenetic Institute, University of Southern California, Los Angeles, California

Abstract

Multiphoton excitation fluorescence microscopy is a powerful noninvasive imaging technique for the deep optical sectioning of living tissues. Its application in several intact tissues is a significant advance in our understanding of organ function, including renal pathophysiological mechanisms. The glomerulus, the filtering unit in the kidney, is one good example of a relatively inaccessible and complex structure, with cell types that are otherwise difficult to study at high resolution in their native environment. In this article, we address the application, advantages, and limitations of this imaging technology for the study of the glomerular filtration barrier and the controversy it recently generated regarding the glomerular filtration of macromolecules. More advanced and accurate multiphoton determinations of the glomerular sieving coefficient that are presented here dismiss previous claims on the filtration of nephrotic levels of albumin. The sieving coefficient of 70-kD dextran was found to be around 0.001. Using a model of focal segmental glomerulosclerosis, increased filtration barrier permeability is restricted only to areas of podocyte damage, consistent with the generally accepted role of podocytes and the glomerular origin of albuminuria. Time-lapse imaging provides new details and important *in vivo* confirmation of the dynamics of podocyte movement, shedding, replacement, and the role of the parietal epithelial cells and Bowman's capsule in the pathology of glomerulosclerosis.

The advanced confocal imaging technique of two- or three-photon, collectively called multiphoton, excitation fluorescence microscopy was established[1] and first applied to the kidney several years ago.[2,3] The basic principles and advantages of the technology, and examples of multiphoton studies in kidney research, have been reviewed previously.[2–8] In this special article, we focus on the application of multiphoton imaging for the study of the glomerular filtration barrier (GFB). Here we briefly discuss select, recent findings in juxtaglomerular physiology that are relevant to the function of the GFB that were obtained using the multiphoton imagingapproach.Then we address the controversy regarding the multiphoton determination of glomerular sieving coefficient (GSC) for macromolecules. New data will be presented using more advanced and accurate multiphoton techniques, suggesting that conventional fluorescence imaging applications have serious limitations for the measurement of GSC and providing evidence that the amount of filtered macromolecules in the Bowman's space is extremely low. Also, time-lapse images and

Correspondence: Dr. János Peti-Peterdi, Department of Physiology and Biophysics and Department of Medicine, Zilkha Neurogenetic Institute, University of Southern California, 1501 San Pablo Street, ZNI 335, Los Angeles, CA 90033. Phone: 323-442-4337; Fax: 323-442-4466; petipete@usc.edu.

Supplemental information for this article is available online at http://www.jasn.org/.

supplementary video material provide new details and important *in vivo* confirmation of podocyte functions in their intact environment during health and disease. These include the dynamics of podocyte migration, shedding, replacement, and the role of the parietal epithelial cells and Bowman's capsule in the puromycin aminonucleoside (PAN) model of focal segmental glomerulosclerosis (FSGS).

MULTIPHOTON IMAGING SHOWS NEW DETAILS OF JUXTAGLOMERULAR FUNCTION

One of the main research interests of our laboratory has been the function of the juxtaglomerular apparatus (JGA), the mechanisms of basic physiologic processes by which cells of the macula densa in the distal nephron control GFR, renal blood flow, and the renin–angiotensin system.[9] Confocal and multiphoton imaging helped to identify new details of the macula densa–mediated, tubular salt/flow–induced afferent arteriole vasoconstriction (tubuloglomerular feedback [TGF])[2,7,8,10,11] and allowed the direct visualization of renin release from the JGA.[8,12,13]

One interesting feature of TGF, which may have great implications for the function of the GFB, is the cell-to-cell calcium signaling that propagates as a calcium wave in the JGA and beyond. Increased salt content or tubular fluid flow at the macula densa triggers elevations in $[Ca^{2+}]$ in the adjacent mesangial and vascular smooth muscle cells, which propagate not only to the afferent arteriole causing vasoconstriction but simultaneously toward all cells of the glomerulus including the most distant podocytes.[11] Although the issue of active podocyte contraction is controversial,[14] elevations in podocyte $[Ca^{2+}]$ and simultaneous reductions in glomerular capillary diameter during TGF[2,11] that exist even in nonperfused glomeruli[11] are consistent with their contractile function *in vivo*. Also well established is the importance of podocyte cell membrane calcium channels (TRPC6 for example) in maintaining normal $[Ca^{2+}]$ dynamics, which produce new pathology, particularly glomerulosclerosis, when dysfunctional.[15]

Propagation of the TGF calcium wave to glomerular podocytes and their involvement in the control of GFR suggests that podocytes may be functionally part of the JGA. Because of the bidirectional propagation of the TGF calcium wave, podocyte $[Ca^{2+}]$ elevations and contractions coincide with afferent arteriole contraction. The timing of this synchronized podocyte contraction is especially interesting because it occurs when intraglomerular capillary pressure is at its lowest. Together with the function of the newly discovered subpodocyte space (SPS) and the oscillatory feature of glomerular function, as detailed below, this raises the possibility that a temporary filter backwash mechanism exists in the GFB that contributes to the maintenance of a clean glomerular filter. Clearly, the location of the major filtration barrier, glomerular basement membrane *versus* the slit diaphragm, and the reasons why the filtration barrier does not clog are still highly debated issues.[16–21] Multiphoton imaging can directly visualize the GFB[16] and the cellular structures of the intact glomerulus in high spatial and temporal resolution *in vivo* and will undoubtedly help to clarify these issues.

The SPS, proposed to be a new layer of the GFB, was discovered and characterized recently by Neal *et al.*[22] The SPS is a labyrinthine fluid space between the underside of podocyte cell body and the foot processes. Subsequent multiphoton imaging studies in the intact glomerulus confirm the findings of these initial morphometric measurements and show that the SPS constitutes a highly significant restriction to flow.[23] The small connectors between the SPS and the Bowman's space, so-called exit pores,[22] may have important functional implications in physiologic (filter backwash, podocyte-to-endothelium crosstalk), as well as pathologic processes (glomerulosclerosis) and needs further study.

Quantitative multiphoton imaging techniques can directly visualize major physiologic functions on the single nephron level, for example, the classic, oscillatory nature of single nephron GFR (SNGFR) and tubular fluid flow.[6] Real-time imaging and measurement of these and other glomerular and tubular functions have been published earlier and are included in supplementary video material.[6,8] For example, regular periods of glomerular contraction–relaxation are observed, resulting in oscillations of filtration (SNGFR) and tubular flow rate. This is measured by changes in fluorescence intensity of the filtered plasma marker 70-kD dextran-rhodamine B in Bowman's space and tubular fluid, as well as by changes in tubular diameter.[6,8] The oscillations clearly show two components: faster (frequency of 0.12 Hz and cycle time about 10 seconds) and slower (frequency of 0.023 Hz and cycle time about 45 seconds) elements that are consequences of the afferent arteriole myogenic and TGF mechanisms, respectively.[24,25]

In addition, real-time multiphoton imaging of the intact kidney *in vivo* confirms the existence of a bulk fluid flow in the JGA interstitium.[26] Using bolus injections of the extracellular fluid marker Lucifer yellow, the rapid ultrafiltration of plasma through fenestrated endothelium in the terminal, renin-expressing segment of the afferent arteriole has been visualized directly.[26] This significant and dynamic fluid flow from the preglomerular vascular lumen to the renal cortical interstitium may be an important source of interstitial macromolecules, in addition to luminal uptake and transcytosis in tubules.[26–28]

CONTROVERSY REGARDING GLOMERULAR SIEVING OF MACROMOLECULES: LIMITATIONS OF THE FLUORESCENCE APPROACH

A few years ago, pioneers in the renal intravital applications of multiphoton imaging made an interesting observation that at the time was a potentially paradigm-shifting discovery regarding the function of the GFB. They observed mass glomerular filtration (high levels of fluorescence in the Bowman's space) of fluorophore-conjugated albumin and 70-kD dextran in normal kidneys (with their glomerular sieving coefficient [GSC] in the range of 0.02 to 0.04) and its rapid endocytosis in the proximal tubule.[27] Based on these multiphoton studies, the authors formulated a hypothesis that the GFB normally leaks albumin at nephrotic levels, and this filtered albumin load is avidly bound and retrieved by cells along the proximal tubule.

This new concept on the tubular origin of proteinuria challenged the old paradigm that proteinuria is of glomerular origin.[15–21,29] The same authors followed up on their initial observation by applying the multiphoton imaging approach in the diabetic kidney and found

basically the same high level of glomerular filtration but failed reabsorption of albumin in the proximal tubule, giving rise to diabetic albuminuria.[28] Because the value of albumin GSC measured by multiphoton microscopy was 50 times greater than previously measured by micropuncture[29] or calculated[30] (GSC in the 0.0006 range), these multiphoton studies generated heated debate in top renal journals.[31–36]

Importantly, two recent independent studies applying the same multiphoton imaging approach to measure the GSC of albumin and 70-kD dextran dismiss previous claims on the filtration of nephrotic levels of albumin by finding that the GSC of albumin and 70-kD dextran were much lower, ~0.002.[35,36] Several technical limitations were identified that were likely responsible for the higher GSC values found by Russo *et al.*,[27] which concerned both poor animal conditions such as hypothermia , dehydration, low BP, and low GFR, as well as imaging-related factors.

Based on earlier work,[37] Tanner[35] identified the high laser outputs (high levels of illumination) and the use of external, instead of internal, photodetectors that were responsible for the collection of significant out-of-focus fluorescence (noise and not albumin) in the Bowman's space in the earlier studies. Other imaging-related factors that led to the flawed GSC measurements by Russo *et al.*[27] include the requirement of higher imaging depth resolution (at least 12-bit as opposed to 8-bit), the significant light scattering by the living kidney tissue, and physiologic heterogeneities in GFB function.[36]

Here we present new multiphoton data (Figure 1) to substantiate our claim that conventional applications of multiphoton microscopy or fluorescence imaging approaches, in general, have serious technical limitations to measuring certain renal functional parameters like GSC. Accurate determination of GSC of albumin or 70-kD dextran *in vivo* requires highly precise measurement of true fluorophore concentrations (fluorescence intensity) in relatively inaccessible compartments such as the glomerular capillary. The kidney's anatomic (dense capillary network, convoluted tubules, fibrous renal capsule) and functional features (high organ blood flow, 20% of cardiac output) make renal tissue especially light absorbing and scattering compared with other organs.[8] Because 20% of plasma is filtered from the glomerular capillaries, the local hematocrit (red blood cell density) is extremely high. In contrast to fluorescence imaging in clear solutions, in glomerular capillaries, the high density of fast moving red blood cells, their significant light absorption caused by hemoglobin content, and scattering caused by high velocity, irregular shape, and deformability result in low efficiency of both fluorophore excitation and detection of emitted fluorescence.[38] This issue is a well-established and important limiting factor for fluorescence imaging applications in several vascular beds, and perhaps the only possible way to prevent it is blood replacement, which yields superior image quality for *in vivo* multiphoton applications.[38]

Figure 1, A through C, shows the high light scattering effect of red blood cells in glomerular capillaries *in vivo*. After taking a single-scan multiphoton image of the intact kidney in Munich-Wistar-Fromter rats as described earlier (Figure 1A),[6,8] the flow of red blood cells was intentionally obstructed in one glomerular capillary loop by a small blood clot, which was formed by briefly focusing the multiphoton excitation laser beam on the luminal surface

of one endothelial cell. This artificially formed thrombus caused no changes in capillary diameter and resulted in only partial capillary occlusion as judged by intact rather than stagnant plasma flow and occasional passage of a few red blood cells in the blood vessel, and it completely dissolved in a few seconds. Figure 1B shows that, when only red blood cell-free clear plasma flows in the same capillary, imaging with the same settings as in Figure 1A results in significantly increased fluorescence intensity of the plasma marker (70-kD dextran). Fluorescence intensity in these studies was measured in regions of interest where plasma fluorescence was the brightest and always at the outer margins of the capillary lumen where blood cell density is the lowest. Similar results are obtained when, without any intervention, the occasional leukocyte sticking and rolling in glomerular capillaries causes the same phenomenon—instantaneous increase in plasma fluorescence (visible in Supplementary Video Material 2). The application of this maneuver results in a three- to fourfold increase in plasma fluorescence; consequently, a much lower GSC is obtained for 70-kD dextran (0.001 ± 0.0004) compared with the control conditions of intact whole blood flow in the capillaries (0.004 ± 0.0004, $n = 11$, $P < 0.05$, using paired t test). Mean arterial BP was monitored throughout imaging and was normal (95 ± 5 mmHg). Thus, accurately performed multiphoton determinations of GSC of albumin and 70-kD dextran provide essentially the same values as established previously by micropuncture.[29]

Another odd finding of the previous measurements by Russo *et al.*[27] was the steady-state level of fluorescence in the Bowman's space. As described before[6,36] and detailed above, and shown in Figure 1D, the physiologic mechanisms of afferent arteriole myogenic tone and TGF cause oscillations in SNGFR consisting of two components, and therefore, the Bowman's space fluorescence is normally nonlinear. Thefailure to detect these characteristic oscillations in Bowman's space fluorescence by these investigators suggests they encountered and measured a high level of nonspecific or background fluorescence.

IMAGING OF PODOCYTE DYNAMICS

We attempted to provide additional multiphoton evidence for the glomerular origin of proteinuria by imaging the morphologic and functional consequences of localized podocyte damage using the experimental model of FSGS. We aimed to find localized elevations in GFB permeability, restricted to areas of podocyte damage, which would argue against the homogenous, nephrotic levels of albumin filtration in glomeruli.[27] Munich-Wistar-Fromter rats were given 100 mg/kg body weight PAN intraperitoneally, as described before, and imaged 4 days after treatment.[39] Animal preparation and fluorophore administration were performed as described earlier,[6] except that Lucifer yellow, a 0.4-kD freely filterable, but cell membrane impermeable, small molecule was infused continuously into the carotid artery (10 μl/min of 12.5 mg/ml stock solution) to label the primary filtrate in the Bowman's space. We found the vascular endothelium and mesangial cells endocytosed Lucifer yellow intensely and consequently were labeled as opposed to normal podocytes and parietal cells that did not show any signs of dye uptake and remained dark and unlabeled during several hours of imaging (Figure 2, Athrough C). It should be noted that the lack of Lucifer yellow and 70-kD dextran endocytosis in podocytes seems to be molecule specific, because previous studies established the endocytosis of albumin and immunoglobulins by these cells.[21,40]

This feature of labeling of the cellular components of GFB gave us a tool to track podocytes in real time based on their lack of labeling. In addition to the images in Figure 2, A through C, a representative video (Supplementary Material 1) shows the movement of one to two podocytes in one thin optical section in a normal untreated glomerulus, whereas most of the other podocytes appear stationary. The few moving podocytes may represent the damaged, activated podocytes that are highly motile as described in a recent review by Mundel and Reiser.[41]

There are several signs that the dark, moving cells cannot be other cell types, for example, a leukocyte. We found that circulating leukocytes are intensely labeled green (visible in supplementary videos) because of their endocytosis of Lucifer yellow, and they are visible as green streaks occasionally passing through the capillary loops. Also, a leukocyte, when sticking and rolling in capillaries, usually blocks the flow of red blood cells; therefore, only plasma can pass through the local narrowing in capillary lumen. However, there is a constant, free flow of red blood cells in the capillary loop that is covered by the moving podocyte, which also appears to be located outside the capillary lumen. Positive identification of podocytes and parietal cells using genetic approaches may provide benefit in future applications. Importantly, Figure 2C shows that all three cell types of the GFB can be visualized not only in Munich-Wistar-Fromter rats but also in the commonly used C57BL6 mouse.

Numerous pseudocysts in podocytes were found after PAN treatment (Figure 2B), consistent with previous reports.[42,43] Using bolus injections of tracer molecules into the carotid artery as described before,[23] the filling and emptying of pseudocysts were studied in time-lapse images (Figure 3). The injected tracer Lucifer yellow appears and clears from Bowman's space very quickly, whereas the filling and emptying in pseudocysts is slightly slower and delayed, similar to what we found earlier in the subpodocyte space.[23] These results suggest the podocyte pseudocysts that form as a result of PAN treatment may represent enlargements of the subpodocyte space.

Because the PAN-induced FSGS is a well-established model of proteinuria, alterations in GFB permeability were assessed by multiphoton measurement of the fluorescence intensity of the plasma marker, 70-kD dextran-rhodamine B, in the Bowman's space. Similarly to the control kidney (Figure 1), a very low level of fluorescence is found in most areas of the Bowman's space (Figure 4, A and B). However, the permeability of the GFB to 70-kD dextran is 5- to 10-fold higher around a damaged, shedding podocyte. A movie of the same preparation is available as Supplementary Material 2, and the leaking plasma marker (high red fluorescence intensity) around the damaged podocyte is clearly visible in contrast to the other, intact capillary loop regions where the Bowman's space is dark. These findings suggest the increased GFB permeability is restricted to areas of podocyte damage, consistent with the old paradigm on the glomerular origin of proteinuria and the key role of podocytes.[15–21,29,39,41] Interestingly, podocyte shedding is always followed immediately by focal thrombus formation in the capillary loop directly underneath the shedding podocyte, which can be explained by the abrupt structural changes of the glomerular basement membrane as a consequence of the damaged podocyte and slit diaphragm as described earlier.[44]

Time-lapse imaging provides details of the dynamics of the shedding and replacement of podocytes *in vivo* in PAN-treated Munich-Wistar-Fromter rats. Figure 5 shows this rather rapid and uniform process. It should be noted that all shedding podocytes exhibit the exact same features and apparently undergo the same process and phases with the same time course as the following. The first sign is always the disappearance of the pseudocyst, followed by the podocyte becoming membrane permeable and consequently highly fluorescence in contrast to the normal, dark podocytes. A small, highly green, autofluorescent punctate region is formed within 2 minutes inside the cell, which gradually became larger. Approximately 6 to 7 minutes after the initial signs, the entire podocyte appears highly green fluorescence and amorphous. After this point, the remaining process is very fast and includes complete podocyte detachment, and in this particular case (shown in Figure 5), its crossing through the parietal Bowman's capsule within 10 seconds. This was, however, a unique finding, because most podocytes simply disappear and end up in the tubular fluid. An elongated, stellate-shaped cell appears quickly from the parietal area of the Bowman's capsule within 10 seconds, which seems to replace the old, detached podocyte within another 50 seconds. A movie of the same preparation is available as Supplementary Material 3. The appearance of the shedding podocyte, the above listed morphologic features, and the rapidity of the process may be consistent with cell necrosis.

The surprising finding that shedding podocytes can break through the parietal Bowman's capsule supports the recent findings of the high permeability and damaged intercellular junctions of parietal cells in glomerular diseases associated with proteinuria.[45,46] Also, multiphoton imaging is able to visualize another interesting function of parietal cells acting as renal progenitor cells that can quickly replace podocytes.[47] Future applications of this imaging approach have great promise and will certainly identify other details of these dynamic processes of podocytes, parietal cells, and the other constituents of the GFB.

CONCLUSION

Multiphoton excitation fluorescence microscopy is an extremely powerful imaging technique for studying the intact kidney with submicrometer resolution. However, fluorescence applications have serious technical limitations for the measurement of certain functional renal parameters such as GSC, which require accurate measurement of fluorophore concentrations (fluorescence intensity) in very small, relatively inaccessible compartments. Nevertheless, more advanced and unconventional uses of the technology find extremely low amounts of filtered macromolecules in the Bowman's space (GSC of 70-kD dextran in the 0.001 range), dismissing previous claims on their mass filtration in the glomerulus. New visual information on intact podocytes, parietal cells, and other elements of the filtration barrier obtained by multiphoton imaging can help to solve the many controversies in glomerular function.

Supplementary Material

Refer to Web version on PubMed Central for supplementary material.

Acknowledgments

DISCLOSURES

This work was supported by National Institutes of Health Grant DK64324 to J.P.P.

REFERENCES

1. Denk W, Strickler J, Webb WW. Two-photon laser scanning fluorescence microscopy. Science. 1990; 248:73–76. [PubMed: 2321027]
2. Peti-Peterdi J, Morishima S, Bell PD, Okada Y. Two-photon excitation fluorescence imaging of the living juxtaglomerular apparatus. Am J Physiol Renal Physiol. 2002; 283:F197–F201. [PubMed: 12060602]
3. Dunn KW, Sandoval RM, Kelly KJ, Dagher PC, Tanner GA, Atkinson SJ, Bacallao RL, Molitoris BA. Functional studies of the kidney of living animals using multicolor two-photon microscopy. Am J Physiol Cell Physiol. 2002; 283:C905–C916. [PubMed: 12176747]
4. Peti-Peterdi J. Multiphoton imaging of renal tissues in vitro. Am J Physiol Renal Physiol. 2005; 288:F1079–F1083. [PubMed: 15883166]
5. Molitoris BA, Sandoval RM. Intravital multiphoton microscopy of dynamic renal processes. Am J Physiol Renal Physiol. 2005; 288:F1084–F109. [PubMed: 15883167]
6. Kang JJ, Toma I, Sipos A, McCulloch F, Peti-Peterdi J. Quantitative imaging of basic functions in renal (patho)physiology. Am J Physiol Renal Physiol. 2006; 291:F495–F502. [PubMed: 16609147]
7. Sipos A, Toma I, Kang JJ, Rosivall L, Peti-Peterdi J. Advances in renal (patho)physiology using multiphoton microscopy. Kidney Int. 2007; 72:1188–1191. [PubMed: 17667980]
8. Peti-Peterdi J, Toma I, Sipos A, Vargas SL. Multiphoton imaging of renal regulatory mechanisms. Physiology (Bethesda). 2009; 24:88–96. [PubMed: 19364911]
9. Schnermann, J.; Briggs, JP. Function of the juxtaglomerular apparatus: Control of glomerular hemodynamics and renin secretion.. In: Alpern, RJ.; Hebert, SC., editors. The Kidney Physiology and Pathophysiology. Elsevier Academic Press; London: 2008. p. 589-626.
10. Thomson SC, Blantz RC. Glomerulotubular balance, tubuloglomerular feedback, and salt homeostasis. J Am Soc Nephrol. 2008; 19:2272–2275. [PubMed: 18322161]
11. Peti-Peterdi J. Calcium wave of tubuloglomerular feedback. Am J Physiol Renal Physiol. 2006; 291:F473–480. [PubMed: 16495210]
12. Peti-Peterdi J, Fintha A, Fuson AL, Tousson A, Chow RH. Real-time imaging of renin release in vitro. Am J Physiol Renal Physiol. 2004; 287:F329–F35. [PubMed: 15082450]
13. Peti-Peterdi J, Harris RC. Macula densa sensing and signaling mechanisms of renin release. J Am Soc Nephrol. 2010; 21:1093–1096. [PubMed: 20360309]
14. Saleem MA, Zavadil J, Bailly M, McGee K, Witherden IR, Pavenstadt H, Hsu H, Sanday J, Satchell SC, Lennon R, Ni L, Bottinger EP, Mundel P, Mathieson PW. The molecular and functional phenotype of glomerular podocytes reveals key features of contractile smooth muscle cells. Am J Physiol Renal Physiol. 2008; 295:F959–F970. [PubMed: 18684887]
15. Winn MP, Conlon PJ, Lynn KL, Farrington MK, Creazzo T, Hawkins AF, Daskalakis N, Kwan SY, Ebersviller S, Burchette JL, Pericak-Vance MA, Howell DN, Vance JM, Rosenberg PB. A mutation in the TRPC6 cation channel causes familial focal segmental glomerulo-sclerosis. Science. 2005; 308:1801–1804. [PubMed: 15879175]
16. Tanner GA, Rippe C, Shao Y, Evan AP, Williams JC Jr. Glomerular permeability to macromolecules in the Necturus kidney. Am J Physiol Renal Physiol. 2009; 296:F1269–1278. [PubMed: 19339627]
17. Farquhar MG. The glomerular basement membrane: Not gone, just forgotten. J Clin Invest. 2006; 116:2090–2093. [PubMed: 16886057]
18. Smithies O. Why the kidney glomerulus does not clog: A gel permeation/diffusion hypothesis of renal function. Proc Natl Acad Sci U S A. 2003; 100:4108–4113. [PubMed: 12655073]
19. Tryggvason K. Unraveling the mechanisms of glomerular ultrafiltration: Nephrin, a key component of the slit diaphragm. J Am Soc Nephrol. 1999; 10:2440–2445. [PubMed: 10541305]

20. Goldberg S, Adair-Kirk TL, Senior RM, Miner JH. Maintenance of glomerular filtration barrier integrity requires laminin alpha5. J Am Soc Nephrol. 2010; 21:579–586. [PubMed: 20150535]
21. Akilesh S, Huber TB, Wu H, Wang G, Hartleben B, Kopp JB, Miner JH, Roopenian DC, Unanue ER, Shaw AS. Podocytes use FcRn to clear IgG from the glomerular basement membrane. Proc Natl Acad Sci U S A. 2008; 105:967–972. [PubMed: 18198272]
22. Neal CR, Crook H, Bell E, Harper SJ, Bates DO. Three-dimensional reconstruction of glomeruli by electron microscopy reveals a distinct restrictive urinary subpodocyte space. J Am Soc Nephrol. 2005; 16:1223–1235. [PubMed: 15829713]
23. Salmon AH, Toma I, Sipos A, Muston PR, Harper SJ, Bates DO, Neal CR, Peti-Peterdi J. Evidence for restriction of fluid and solute movement across the glomerular capillary wall by the subpodocyte space. Am J Physiol Renal Physiol. 2007; 293:F1777–F1786. [PubMed: 17804486]
24. Holstein-Rathlou N-H, Leyssac PP. TGF-mediated oscillations in proximal intratubular pressure: Differences between spontaneously hypertensive rats and Wistar-Kyoto rats. Acta Physiol Scand. 1986; 126:333–339. [PubMed: 3962682]
25. Marsh DJ, Sosnovtseva OV, Chon KH, Holstein-Rathlou NH. Nonlinear interactions in renal blood flow regulation. Am J Physiol Regul Integr Comp Physiol. 2005; 288:R1143–R1159. [PubMed: 15677526]
26. Rosivall L, Mirzahosseini S, Toma I, Sipos A, Peti-Peterdi J. Fluid flow in the juxtaglomerular interstitium visualized in vivo. Am J Physiol Renal Physiol. 2006; 291:F1241–F1247. [PubMed: 16868308]
27. Russo LM, Sandoval RM, McKee M, Osicka TM, Collins AB, Brown D, Molitoris BA, Comper WD. The normal kidney filters nephrotic levels of albumin retrieved by proximal tubule cells: Retrieval is disrupted in nephrotic states. Kidney Int. 2007; 71:504–513. [PubMed: 17228368]
28. Russo LM, Sandoval RM, Campos SB, Molitoris BA, Comper WD, Brown D. Impaired tubular uptake explains albuminuria in early diabetic nephropathy. J Am Soc Nephrol. 2009; 20:489–494. [PubMed: 19118149]
29. Tojo A, Endou H. Intrarenal handling of proteins in rats using fractional micropuncture technique. Am J Physiol. 1992; 263:F601–F606. [PubMed: 1415732]
30. Lazzara MJ, Deen WM. Model of albumin reabsorption in the proximal tubule. Am J Physiol Renal Physiol. 2007; 292:F430–F439. [PubMed: 16954345]
31. Christensen EI, Birn H, Rippe B, Maunsbach AB. Controversies in nephrology: Renal albumin handling, facts, and artifacts! Kidney Int. 2007; 72:1192–1194. [PubMed: 17805237]
32. Comper WD, Haraldsson B, Deen WM. Resolved: Normal glomeruli filter nephrotic levels of albumin. J Am Soc Nephrol. 2008; 19:427–432. [PubMed: 18216311]
33. Gekle M. Renal albumin handling: A look at the dark side of the filter. Kidney Int. 2007; 71:479–481. [PubMed: 17344895]
34. Remuzzi A, Sangalli F, Fassi A, Remuzzi G. Albumin concentration in the Bowman's capsule: Multiphoton microscopy vs micropuncture technique [Letter]. Kidney Int. 2007; 72:1410–1411. [PubMed: 18004314]
35. Tanner GA. Glomerular sieving coefficient of serum albumin in the rat: A two-photon microscopy study. Am J Physiol Renal Physiol. 2009; 296:F1258–F1265. [PubMed: 19211688]
36. Peti-Peterdi J. Independent two-photon measurements of albumin GSC give low values. Am J Physiol Renal Physiol. 2009; 296:F1255–F1257. [PubMed: 19297453]
37. Theer P, Denk W. On the fundamental imaging-depth limit in two-photon microscopy. J Opt Soc Am A Opt Image Sci Vis. 2006; 23:3139–3149. [PubMed: 17106469]
38. Haiss F, Jolivet R, Wyss MT, Reichold J, Braham NB, Scheffold F, Krafft MP, Weber B. Improved in vivo two-photon imaging after blood replacement by perfluorocarbon. J Physiol. 2009; 587:3153–3158. [PubMed: 19403621]
39. Kim YH, Goyal M, Kurnit D, Wharram B, Wiggins J, Holzman L, Kershaw D, Wiggins R. Podocyte depletion and glomerulosclerosis have a direct relationship in the PAN-treated rat. Kidney Int. 2001; 60:957–968. [PubMed: 11532090]
40. Eyre J, Ioannou K, Grubb BD, Saleem MA, Mathieson PW, Brunskill NJ, Christensen EI, Topham PS. Statin-sensitive endocytosis of albumin by glomerular podocytes. Am J Physiol Renal Physiol. 2007; 292:F674–F681. [PubMed: 17032937]

41. Mundel P, Reiser J. Proteinuria: an enzymatic disease of the podocyte? Kidney Int. 2010; 77:571–580. [PubMed: 19924101]

42. Yoshikawa N, Ito H, Akamatsu R, Hazikano H, Okada S, Matsuo T. Glomerular podocyte vacuolation in focal segmental glomerulo-sclerosis. Arch Pathol Lab Med. 1986; 110:394–398. [PubMed: 3754422]

43. Gassler N, Elger M, Kränzlin B, Kriz W, Gretz N, Hähnel B, Hosser H, Hartmann I. Podocyte injury underlies the progression of focal segmental glomerulosclerosis in the fa/fa Zucker rat. Kidney Int. 2001; 60:106–116. [PubMed: 11422742]

44. Fissell WH, Hofmann CL, Ferrell N, Schnell L, Dubnisheva A, Zydney AL, Yurchenco PD, Roy S. Solute partitioning and filtration by extracellular matrices. Am J Physiol Renal Physiol. 2009; 297:F1092–F1100. [PubMed: 19587146]

45. Ohse T, Chang AM, Pippin JW, Jarad G, Hudkins KL, Alpers CE, Miner JH, Shankland SJ. A new function for parietal epithelial cells: A second glomerular barrier. Am J Physiol Renal Physiol. 2009; 297:F1566–F1574. [PubMed: 19794110]

46. Ohse T, Pippin JW, Chang AM, Krofft RD, Miner JH, Vaughan MR, Shankland SJ. The enigmatic parietal epithelial cell is finally getting noticed: A review. Kidney Int. 2009; 76:1225–1238. [PubMed: 19847153]

47. Ronconi E, Sagrinati C, Angelotti ML, Lazzeri E, Mazzinghi B, Ballerini L, Parente E, Becherucci F, Gacci M, Carini M, Maggi E, Serio M, Vannelli GB, Lasagni L, Romagnani S, Romagnani P. Regeneration of glomerular podocytes by human renal progenitors. J Am Soc Nephrol. 2009; 20:322–332. [PubMed: 19092120]

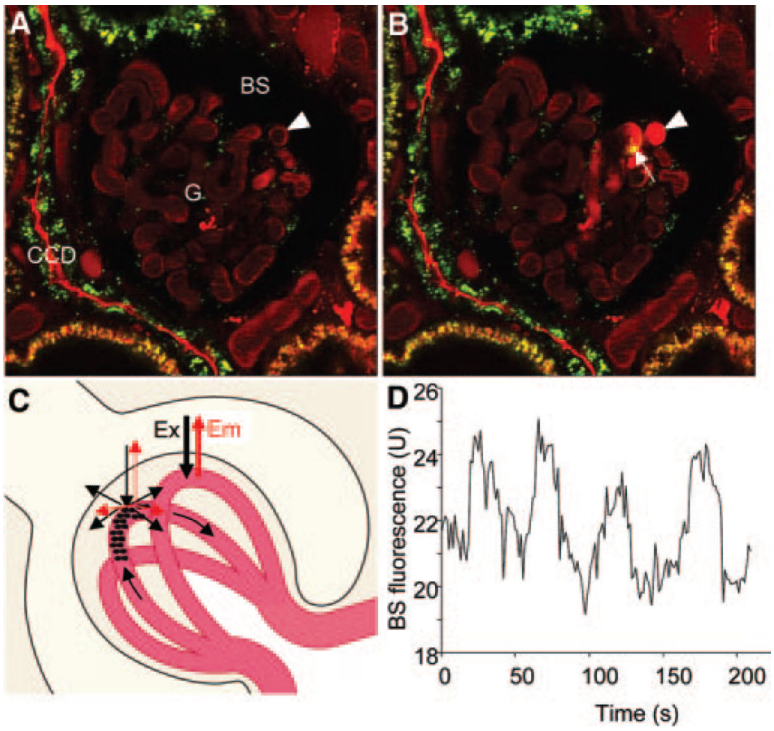

Figure 1.

Limitations of the multiphoton fluorescence imaging approach when measuring glomerular sieving of macromolecules. (A) *In vivo* multiphoton image of an intact glomerulus (G) from a Munich-Wistar-Fromter rat. The intravascular space (plasma) is labeled red using 70-kD dextran-rhodamine B. Red blood cells appear in high density as unlabeled, dark objects in the capillary lumen. A minor, invisible fraction of 70-kD dextran is filtered into the Bowman's space (BS), and it becomes highly concentrated (fluorescence) in the tubular lumen of the cortical collecting duct (CCD). Note the relatively low level of red fluorescence in the glomerular capillary lumen. However, when only red blood cell-free, clear plasma flows in a capillary loop (B, arrowhead, the same glomerulus is shown as in A using the same imaging settings), the plasma fluorescence increases significantly. The flow of red blood cells was obstructed by a small blood clot (arrow), which was formed temporarily in response to briefly focusing the multiphoton laser beam on the luminal surface of one endothelial cell upstream in the glomerular capillary. (C) Illustration of the highly light absorbing and scattering effect of red blood cells streaming in the capillary lumen in high density that results in low efficiency of fluorophore excitation (Ex) and detection of emitted fluorescence (Em). In contrast, the excitation and fluorescence detection are highly efficient in clear solutions (red blood cell-free capillary). (D) Recording of low levels of rhodamine B-fluorescence in the Bowman's space (BS). The level of fluorescence intensity is not steady state; normally, it shows regular oscillations.

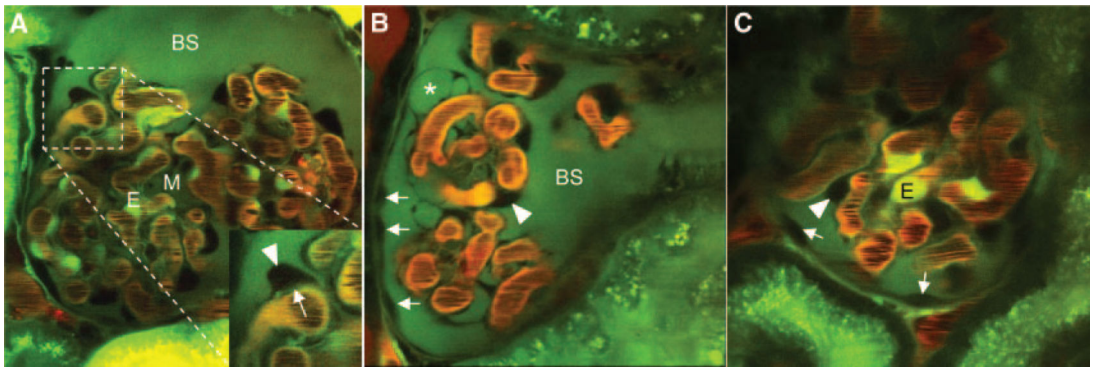

Figure 2.

Multiphoton images of glomeruli *in vivo* in (A) control or (B) PAN-treated Munich-Wistar-Fromter rat and (C) control C57BL6 mouse kidneys. The intravascular space (plasma) marker 70-kD dextran-rhodamine B (red) was given in bolus, and Lucifer yellow, a 0.4-kD easily filterable, but cell membrane impermeable, small molecule (green) was infused continuously into the carotid artery to label the primary filtrate in the Bowman's space (BS) green. The vascular endothelium (E) and mesangial cells (M) are intensely labeled green-yellow because they readily endocytose Lucifer yellow as opposed to podocytes (arrowhead, enlarged in inset in A) and parietal cells (arrow) that normally do not and therefore remain unlabeled (dark, negative image). (B) Numerous pseudocysts under the podocytes (asterisk) are clearly visible after PAN treatment.

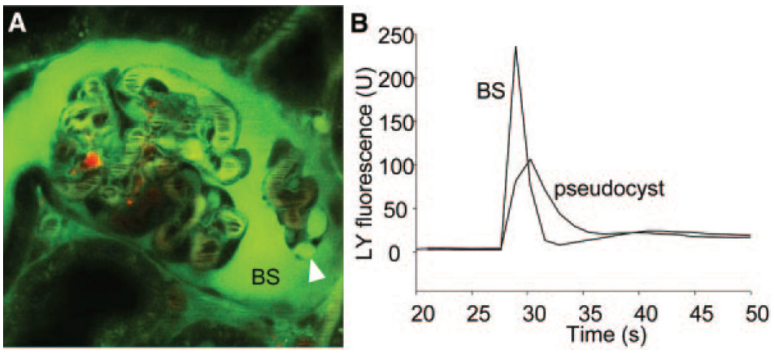

Figure 3.

Podocyte pseudocysts that form as a result of PAN treatment are enlargements of the subpodocyte space. (A) *In vivo* multiphoton image of an intact glomerulus from a PAN-treated Munich-Wistar-Fromter rat. The intravascular space (plasma) is labeled red using 70-kD dextran-rhodamine. (B) Lucifer yellow was injected into the carotid artery in bolus, and the time-lapse of its fluorescence (green) was recorded in the Bowman's space (BS) and inside pseudocysts (arrowhead) as shown in A. Lucifer yellow appeared and cleared from the BS quickly, whereas the filling and emptying in pseudocysts were slightly slower and delayed.

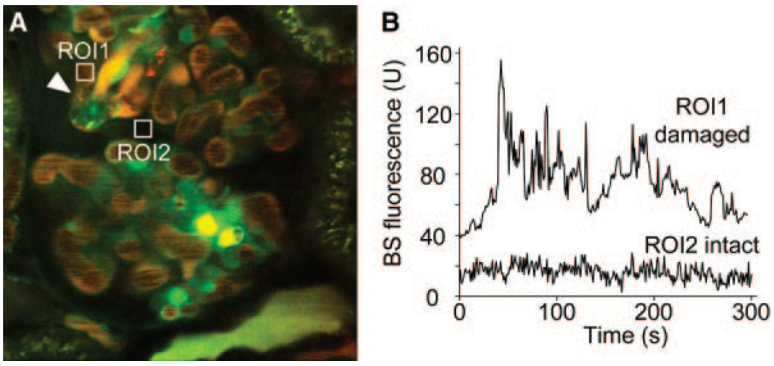

Figure 4.

Increased GFB permeability is restricted to areas of podocyte damage. (A) *In vivo* multiphoton image of a glomerulus from a PAN-treated Munich-Wistar-Fromter rat. The intravascular space (plasma) is labeled red using 70-kD dextran-rhodamine. (B) Cell nuclei are labeled weakly using Hoechst33342 and a green filter. The time-lapse of rhodamine B fluorescence was recorded in the Bowman's space (BS) as shown in A in two regions of interest: around a damaged, shedding podocyte (arrowhead, ROI1) and around an intact capillary loop (ROI2). GFB permeability to 70-kD dextran was 5- to 10-fold higher around a damaged podocyte. Focal thrombus formation is visible in the capillary loop directly underneath the shedding podocyte.

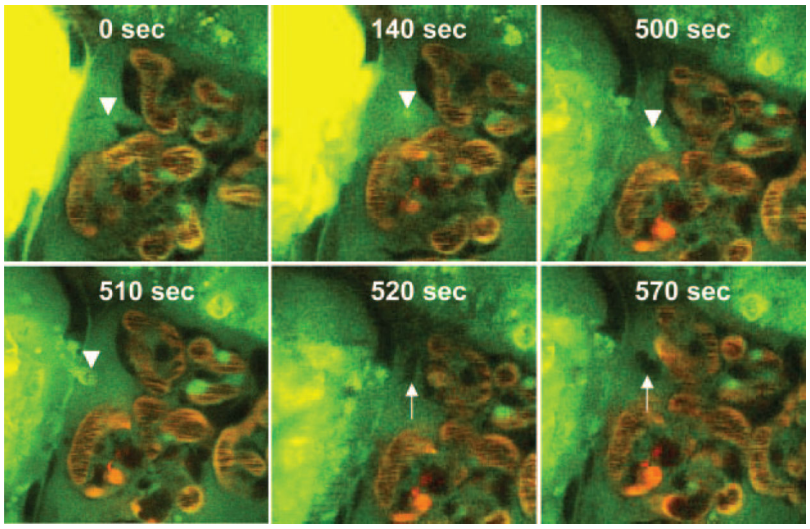

Figure 5.

Time-lapse imaging of the shedding and replacement of podocytes *in vivo* in PAN-treated Munich-Wistar-Fromter rats. The intravascular space (plasma) marker 70-kD dextran-rhodamine B (red) was given in bolus, whereas Lucifer yellow was continuously infused into the carotid artery to label the Bowman's space and visualize podocytes by their lack of labeling (dark cells). Time-series images show the detachment of a pseudocyst-containing podocyte (arrowhead) off of the glomerular capillary wall, its leaving the glomerulus by breaking through the parietal Bowman's capsule, and quick replacement by another newly recruited cell (arrow). After the disappearance of the pseudocyst, the amorphous, detaching podocyte becomes membrane-permeable and highly fluorescence (visible at 500 seconds). After this point, the remaining process is very fast, including complete podocyte detachment and its crossing through the parietal Bowman's capsule within 10 seconds and the appearance of an elongated, stellate-shaped cell (arrow) from the parietal area of the Bowman's capsule within another 10 seconds. Within another 50 seconds, this new cell appears to replace the old, detached podocyte.